A Data-Driven Approach to Artificial Pancreas Verification and Synthesis.

Taisa Kushner*, David Bortz*, David M. Maahs†, and Sriram Sankaranarayanan*.
* University of Colorado, Boulder, CO, USA. **Email:** firstname.lastname@colorado.edu
† Stanford University School of Medicine, Stanford, CA, USA. **Email:** dmaahs@stanford.edu

***Abstract*—This paper presents a case study of a data driven approach to verification and parameter synthesis for artificial pancreas control systems which deliver insulin to patients with type-1 diabetes (T1D). We present a new approach to tuning parameters using non-deterministic data-driven models for human insulin-glucose regulation, which are inferred from patient data using multiple time scales. Taking these equations as constraints, we model the behavior of the entire closed loop system over a five-hour time horizon cast as an optimization problem. Next, we demonstrate this approach using patient data gathered from a previously conducted outpatient clinical study involving insulin and glucose data collected from 50 patients with T1D and 40 nights per patient. We use the resulting data-driven models to predict how the patients would perform under a PID-based closed loop system which forms the basis for the first commercially available hybrid closed loop device. Futhermore, we provide a re-tuning methodology which can potentially improve control for 82% of patients, based on the results of an exhaustive reachability analysis. Our results demonstrate that simple nondeterministic models allow us to efficiently tune key controller parameters, thus paving the way for interesting clinical translational applications.**

I. Introduction

Type-1 Diabetes (T1D), a condition affecting millions of individuals, is treated by external delivery of insulin to keep the blood glucose levels in an acceptable range. However, the insulin dosing decision is currently manual, placing a high burden on the patient. Artificial pancreas (AP) controllers that automatically adjust insulin delivery to maintain blood glucose levels within acceptable ranges promise to improve quality of life and reduce potential complications [6], [10]. However, the AP is a safety-critical system with excess insulin risking the patient to coma or even death.

The control algorithms used in the artificial pancreas rely on parameters such as gains and thresholds which affect the safety and performance of the closed-loop system. At the same time, patients with T1D exhibit a large range of variations in relevant physiological characteristics such as gender, weight, and insulin sensitivity, all of which affect their response to blood glucose levels. Thus, a parameter setting that is safe for person A may be dangerous for person B. Personalization requires the careful tuning of parameters to ensure safety and optimal control performance for a given patient.

Many AP control algorithms have been proposed, at various stages of clinical trials [28]. Recently, the US FDA approved the Medtronic 670G system that uses a PID-based control algorithm [19], [23], [45], [48]. However, the tuning process presents the greatest challenge for translating the artificial pancreas from the laboratory to the general market. Currently, the tuning practice is performed manually by clinicians using a rule of thumb (eg., divide the person's daily insulin dose by 135). Unfortunately, despite this guideline, physicians still spend months manually re-tuning the controller in a guess-and-check method. This process is a large time burden on the physician and patient, and leaves significant room for human error. While there is ongoing work to determine efficacy of one control scheme over another, to our knowledge, very little work has been done to verify safety of parameter settings on a patient-by-patient basis [5], [6], [9], [30], [46].

In this work, we present an approach that integrates data-driven modeling with reachability analysis to analyze the efficacy of the tuning procedure for the PID-based AP controller proposed by Steil et al [45], [48], [50], which forms the basis for the commercial product [1]. Using data from an unrelated outpatient study of a *different* AP controller proposed by Cameron et al [8], [34], we construct linearized data-driven models that predict a range of possible glucose values accounting for the modeling and measurement uncertainties. Furthermore, rather than use a single model, we combine the outputs of multiple models that use different parts of the patient's historical blood glucose and insulin values. Next, we perform reachability analysis on the resulting models in closed loop with the PID control scheme taken from the literature. This allows us to try various parameter values for the controller against the data driven models. Thus, we derive a new, concise, and patient-specific parameter tuning methodology for the PID controller proposed by Steil et al. Our approach predicts that the new methodology will significantly improve the overall control for 83% of the patients in the dataset.

Contributions: (a) We present a data-driven modeling and verification framework applied to model the artificial pancreas, and perform worst-case analysis on closed loop controllers. Our approach reproduces interesting trends in controller efficacy across patients that have been discussed in the clinical literature. (b) We use the results to quantitatively predict how the controller would behave on existing patients. (c) Finally, we use the results of our analysis to derive useful rules of thumb which seem to provide improved safety and control

[1]However, the exact relationship between the academic versions and the commercially approved product is not known to us.

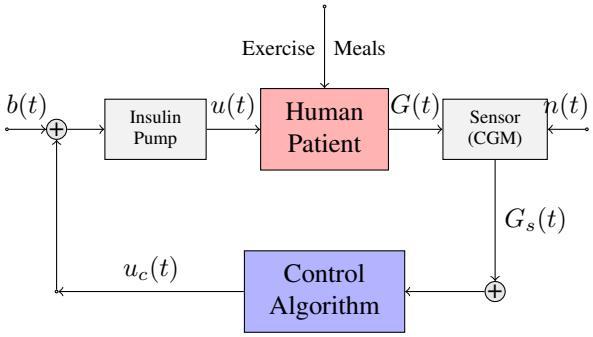

Fig. 1: Overview of the key components of an artificial pancreas control system. $b(t)$: external insulin, $u(t)$: insulin infused, $G(t)$: BG level, $n(t)$: measurement error, $G_s(t)$: sensed glucose level, $u_c(t)$: insulin infusion commanded.

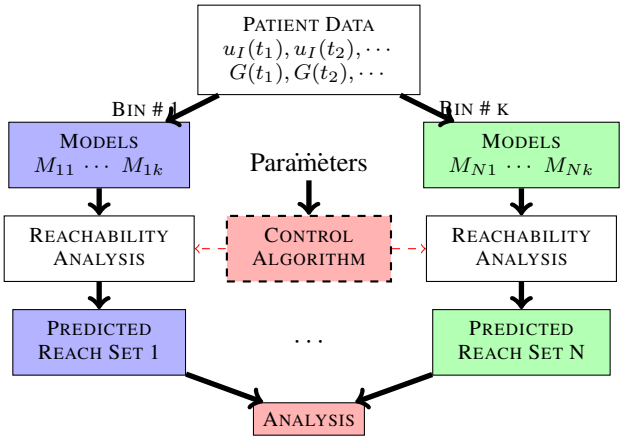

Fig. 2: Overview of the proposed approach to data driven modeling and parameter synthesis for tuning controllers.

performance. These rules have the potential for translating to clinical applications.

II. Background And Motivation

In this section, we will briefly summarize the relevant background on artificial pancreas control systems and motivate the need for a personalized, data-driven approach to verification and parameter synthesis. Further details are available from a variety of surveys and textbooks [10], [11], [47].

Artificial Pancreas: The artificial pancreas (AP) controller regulates the external delivery of insulin to people with T1D. Insulin is a hormone naturally secreted by the pancreas in people without T1D, and by various means lowers the blood glucose (BG) levels. Figure 1 shows a simplified closed loop diagram for the artificial pancreas. The system delivers insulin through a pump that can be commanded by the control algorithm to deliver varying amounts of insulin over time. BG levels are sensed using a continuous glucose monitor (CGM). Together, the pump and the CGM, along with possibly other inputs such as (impending) meal and exercise announcements, form a closed loop that seeks to maintain the patient's BG levels inside a *euglycemic* range of $[70, 180]$ mg/dL. If the BG levels fall below 70 mg/dL, the resulting condition is called *hypoglycemia*. This is a dangerous condition that can lead to loss of consciousness, coma or even death. On the other hand, levels above 180 mg/dL are called *hyperglycemia*. They pose longer term dangers such as damage to organs such as kidneys, heart, eyes, nerves and peripheral blood vessels. Extremely high levels, ≥ 300 mg/dL, lead to a condition called *ketacidosis*, which requires immediate emergency care.

Numerous AP algorithms have been proposed, and are under various stages of clinical evaluation [28]. Major categories include PID control algorithms [45], [48]–[50], model-predictive control (MPC) algorithms [4], and fuzzy rule-based controllers [3], [29]. The systems are further classified as night-time only versus full 24 hour control; insulin-only control algorithms versus control algorithms that combine insulin with the counter-regulatory hormone glucagon [16] and finally algorithms that vary in how much human inputs they assume – these range from hybrid closed loops that augment manual control [8], [23], [50] to a fully automated closed loop [7], [18], [24].

A. Insulin-Glucose Regulation Models

A large variety of models have been proposed for modeling how blood glucose levels respond to insulin and meal inputs [14], [26], [32], [35], [36], [39], [51]. In particular, the high-fidelity UVA-Padova model, relies on system of ODEs with 10 variables and nearly 40 patient parameters [36]. This model has been approved for pre-clinical trials by the US FDA [43]. Parameter sets representing virtual patients are available based on measurements from real patients [13]. However, for data driven approaches, these models suffer from two drawbacks: (a) the state variables of the model are not directly observable without highly intrusive measurements [12]; and (b) the parameters are not uniquely identifiable from the available data which consists of BG levels and insulin.

In contrast, we use data driven models that predict future glucose values as a function of past glucose and insulin values. This data-driven approach provides an alternative framework for inferring governing glucose-insulin dynamics using data that physicians already have on-hand for their patients with diabetes. Such data-driven modeling approaches are common in many fields including biological systems, spatio-temporal systems, along with the simpler temporal systems, and hence provide a robust framework for our work [31], [37], [38], [44]. Ghorbani et al propose data driven models using ideas from fractional calculus and derive control strategies from their models [20]. In contrast, we propose an approach that uses linear but non-deterministic models: i.e., the models predict a range of possible future BG values rather than a single value. Such a model also accounts for uncertainties that include sensor noise, modeling errors and unmodeled externalities.

B. Proposed Approach

Figure 2 shows the overall flow of the proposed approach. Starting from "longitudinal data" from a single patient over a suitably long period of time that includes insulin and CGM sensor readings, we first construct a set of mathematical models by partitioning the data into bins, wherein each bin yields a set of models. The resulting models are non-deterministic in nature: i.e., they predict a range of possible BG values rather than a single point prediction. Next, we analyze these predictive models and a control algorithm to close the loop to predict all possible reachable sets of states over a given time horizon. This process allows us to "tune" parameters by systematically comparing how different parameter values behave with respect to these models. Finally, we split patients into test and training groups, and identify and test a re-tuning rule based on our models and individual physiology following a k-fold cross-validation protocol.The proposed modeling and synthesis approach has four aspects:

Nondeterministic Models: we construct models that predict intervals rather than points. These intervals seek to account for the noisy BG measurements, modeling errors and the effects of unknown externalities.

Multi Timescale Models: we will consider the combination of multiple models each with a different time scale. This is natural in many physiological applications wherein the control inputs (drugs) have a longer term influence on the physiological quantity predicted.

From Models to Constraints: we will treat each model as providing a constraint on a future BG value. We will combine these models naturally inside an optimization formulation to design reachability analysis algorithms that can predict the future range of BG values under a given control algorithm. Specifically, for the PID controller with saturation and anti-windup compensation proposed by Steil et al [19], [45], [48], [50], the optimization problem reduces to an integer linear program that can be efficiently solved by modern solvers.

Improved Tuning Methodology: we split patients into training and test sets, and combine our models and reachability results with clustering and regression analysis to develop a methodology for identifying improved parameter settings. We follow best-practices of statistical analysis and perform k-fold cross validation.

III. Data-Driven Modeling

In this section, we describe and justify our approach to data driven modeling.

A. Patient Data

We obtained data from a home trial of a predictive pump shutoff system for $n = 50$ anonymous patients with T1D. For each patient, the dataset contains 40 overnight sessions for each patient [8], [34]. For each nightly session, we obtain CGM readings at one minute intervals along with a detailed log of the insulin delivered through the night via the pump. The data also records adverse hypoglycemia events that required treatment using "rescue carbohydrates". Such nights were omitted from consideration for our modeling purposes, since details on the amount of carbohydrates are not available. The dataset does *not* include meals, exercise, or insulin history prior to the start of the recorded nightly sessions, nor is daytime data available. In order to avoid confounding our analysis with residual effects of meals, or exercise, which can persist for multiple hours, we remove the first 180min of nightly data. This allows us to deduce base glucose-insulin dynamics and to calculate insulin-on-board, as explained in the following subsection, [III-B].

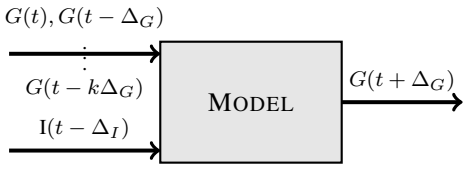

Fig. 3: The overall model structure for a model that predicts the value of glucose $t + \Delta_G$ time into the future, using the past history of insulin and glucose inputs.

B. Model Structure

Figure 3 shows the desired overall structure of the model. The inputs to the model at time t include the history of insulin and glucose levels of the patient, and the output includes a future predicted glucose level at some time $t + \Delta_G$. However, a key problem lies in understanding what portion of the history is relevant to the model as a whole. Doing so helps us avoid overfitting to the data and also control for unknown patient activity such as meal and exercise.

Insulin-On-Board: Insulin is typically administered under the skin and thereafter, is absorbed into the blood and transported to the tissues where it affects glucose uptake. Additionally, insulin has an *action profile* that includes a 20 minute delay before beginning action, a peak action time of 75 minutes and a duration of insulin action of 180 minutes. Thus, to understand the impact of past insulin, we need to convolve the insulin infused with the assumed action profile to obtain a quantity called the (active) insulin on board (IOB). Calculating the IOB requires us to understand the action profile of insulin on a particular patient, which can be quite intrusive [12]. Therefore, the IOB is calculated on a "typical" (somewhat idealized) population level action profile curve. For the purposes of this paper, we will use the calculation provided in the open source artificial pancreas system [41]. Let t be the current time, δ be a small time duration (taken to be one minute in our calculations), and let $u_I(t - k\delta)$ represent the insulin infused in the time interval $(t - (k-1)\delta, t - k\delta]$. The IOB at time t (denoted $\mathrm{I}(t)$) is calculated using the formula

$$\begin{array}{l}\sum_{k=1}^{k_p} u_I(t-k\delta)(1 - 7.4\times10^{-5}k^2\delta^2 + 3.75\times10^{-4}k\delta) \\ +\sum_{k=k_p+1}^{k_d} u_I(t-k\delta)(0.56 - 0.011k\delta + 5.3\times10^{-5}k^2\delta^2)\end{array} \quad (1)$$

Here $k_p\delta$ is the peak action time and $k_d\delta$ is the duration of action, taken to be 75 and 180 minutes in our calculation. Note that the value of $\mathrm{I}(t)$ can be calculated for any t wherein

we have 180 minutes of past insulin data. Thus, our models consider $\mathrm{I}(t)$ instead of the raw insulin input.

Partitioning the Dataset: First, we partition the available dataset into bins wherein the model construction and the resulting analysis are performed for the data in each bin. Such a partitioning allows us to use simpler models inside each bin, and mitigates against physiological factors that vary over time and can influence the resulting glucose values. We adopt a simple binning strategy where each nightly session is partitioned into time windows of T minutes of data. We consider $T \in \{120, 180, 300\}$minutes, deriving models for all three choices of bin sizes.

Next, for each bin, we consider multiple models, each of which is a linear ARMAX-based model that predicts a future range of BG levels using a carefully selected part of the part glucose and insulin (IOB) data.

ARMAX Models: Our approach is based on a well known linear modeling approach, *auto-regressive moving average state-space* models. Given a discrete-time process with past states $x(t), x(t-1), \ldots,$ and inputs $u(t), u(t-1), \ldots,$ an ARMAX model has the form:

$$x(t+1) = \sum_{i=0}^{p-1} a_i x(t-i) + \sum_{j=0}^{q-1} b_i u(t-j) + e(t)\,,$$

wherein $a_0, \ldots, a_{p-1}$ represent the coefficients of the "auto-regressive" part of the model, $b_0, \ldots, b_{q-1}$ represent the "moving average" part of the model and $e(t) \simeq 0$ is the prediction error. ARMAX models are a well studied approach to data driven modeling for process data, with efficient algorithms for finding optimal models [27], [40]. Furthermore, the theory behind ARMAX model allows a systematic approach to selecting an optimal history size for (p, q) using criteria such as the Akaike Information Criterion (AIC) and Partial Autocorrelation (PACF) [2], [22], [33]. Our approach will use ARMAX-based models of the form

$$G(t+\Delta_G) \in a_0 G(t) + a_1 G(t-\Delta_G) + b\ \mathrm{I}(t-\Delta_I) + [L, U]\,.$$

For our purposes, we have extended the ARMAX framework to incorporate two time series, glucose and insulin. Our model consists of a linear combination of historical glucose data (the auto-regressive ARMAX term), historical insulin data (akin to the moving-average ARMAX terms), plus an uncertainty interval $[L, U]$. Such a model maps predicts an interval of possible values rather than a single value. We use a single value of IOB input in our model since the IOB already represents an aggregation of past insulin values. We identify a parsimonious model order of $p = 2$ by computing the partial autocorrelation, PACF, value for various combinations of Δ_G, Δ_I across all patients and trial nights. For all cases $\Delta_G = 5, 30, 45, 60$, we found the first two lags to be the strongest predictors of future glucose values (see Table I).

Additionally, we incorporate the following constraints, using known facts from the physiology of glucose and insulin [10]:

1) The future value of glucose is positively correlated with the past values. i.e, $a_0, a_1 > 0$.
2) The model is close to being marginally stable, though not precisely so. i.e, $a_0 + a_1 \simeq 1$. This is enforced by adding a penalty term $(a_0 + a_1 - 1)^2$ to the model fitting process.
3) Insulin has a inhibitory effect on the value of glucose. $b < 0$.

Rank	Mode lag number for Δ_G (percent occurrence)			
	5min	30min	45min	60min
1	1 (70%)	1 (87%)	1 (83%)	1 (100%)
2	2 (73%)	2 (80%)	2 (70%)	2 (77%)
3	2 (13%)	10 (20%)	2 (27%)	4 (30%)
4	60 (10%)	4 (23%)	4 (27%)	4 (40%)
5	53 (10%)	6 (20%)	4 (33%)	3 (43%)

TABLE I: Table showing top 5 values for j for the correlation of $G(t - j\Delta_G)$ with $G(t)$ over the dataset. Selecting $p = 2$ yields a strong PACF value for predicting future glucose values in over 70% of all bins, whereas there is a drastic drop in significance of $p \geq 3$.

Model Fitting: For fixed values of the delays Δ_G, Δ_I, the model coefficients a_0, a_1, b are computed as the optimal solution to the following optimization problem:

$$\begin{array}{ll} \mathsf{min} & \sum ||e(t)||_2^2 + \lambda(a_0 + a_1 - 1)^2 \\ \mathsf{s.t.} & a_0 > 0, a_1 > 0, b < 0 \end{array}$$

wherein $e(t)$ is the residual at time t computed as

$$e(t) = G(t+\Delta_G) - a_0 G(t) - a_1 G(t-\Delta_G) - b\mathrm{I}(t-\Delta_I)\,,$$

and $\lambda \in (0, 1)$ is a regularization factor. This is a quadratic optimization problem that can be solved using widely available off-the-shelf software.

Confidence Intervals: Once a model is fit for the given data and values of Δ_G, Δ_I, we collect the values of the residuals $e(t)$ for each data point at time t. The empirical range of residuals $[\min_t e(t), \max_t e(t)]$ estimates all the observed residual values. We compute a 99% confidence interval $[L, U]$ over the distribution of the residuals by first computing the mean μ and standard deviation σ. We compute $[L, U] : \ [\mu - 4\sigma, \mu + 4\sigma]$. Using the Chebyshev-Cantelli inequality, we note that $\mathbb{P}(|X - \mu| \geq 4\sigma) \leq \frac{1}{16}$. However, in practice we observe that the residuals fit a tigher-than-Gaussian distribution and thus, the 4σ interval chosen subsumes the empirical range of residual values.

Composite Model with Multiple Time Scales: Next, we address the question of choosing the time delays Δ_G for BG and Δ_I for the IOB term. Once again, the choice may be dictated by a model selection criterion such as the AIC. However, an alternative approach is to allow multiple possible values for (Δ_G, Δ_I) informed by the commonly assumed durations for onset of insulin action, peak action and total duration of action, leading to multiple models that are held to be simultaneously correct. For example, one possible set of combinations could include

$$(\Delta_G, \Delta_I) \in \{(30, 60)(45, 45), (60, 30), (75, 15), (90, 0)\}$$

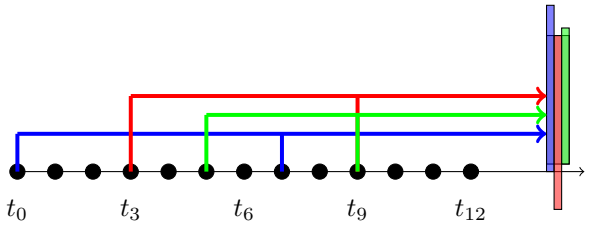

Fig. 4: Figure illustrating the prediction of a composite model using three different ARMAX models with different combinations of (Δ_G, Δ_I) values obtained as the intersection of the individual interval ranges predicted by each model.

yielding 5 different models that predict the future values of BG based on *selecting different parts* of the historical data. The interval predicted by the composite model at some time point t is taken to be the intersection of the intervals for each of the individual models, as illustrated by Figure 4.

However, there is a drawback in doing so. Since each model predicts an interval that has 99% confidence, the probability that the BG value may lie outside the intersection of the predicted intervals will be larger than 1%. Using Boole's inequality, we note that a composite model made up of 5 individual models with 99% confidence will yield an interval with *at least* 95% confidence.

Thus, the composition of multiple models trades off finding a smaller interval but at the loss of confidence that the predicted value will lie within the composite model's interval. Since the regression process allows us to choose the interval to achieve a desired confidence, it is often desirable to choose this confidence and the number of models so that the resulting composite model has at least 95% confidence.

Finally, we note that in theory, the models may be *inconsistent* i.e, the intersection of the intervals predicted by the different models may be empty, since we ascribe a small probability that the actual value may lie outside the predicted interval. We note that such inconsistency has not been observed on the models inferred using the currently available patient data.

Illustrative Example: As an illustrative example, the following models were obtained for a single bin consisting of 6 hours of data for patient ID 1 from the very first overnight session.

$$
\begin{aligned}
G(t+5) &\in G(t) + [-10, 10] \\
G(t+30) &\in 0.29G(t-30) + 0.81G(t) \ldots \\
&\quad - 10.98\mathrm{I}(t-30) + [-41.50, 39.86] \\
G(t+45) &\in 0.46G(t-45) + 0.69G(t) \ldots \\
&\quad - 15.86\mathrm{I}(t-45) + [-39.77, 38.57] \\
G(t+60) &\in 0.58G(t-60) + 0.62G(t) \ldots \\
&\quad - 16.08\mathrm{I}(t-60) + [-28.22, 27.76] \\
G(t+120) &\in 0.37G(t-120) + 0.78G(t) \ldots \\
&\quad - 17.12\mathrm{I}(t-120) + [-18.89, 18.71]
\end{aligned}
$$

$$
\begin{aligned}
I_e(t) &= I_e(t-5) + (G(t) - G_0) \quad \leftarrow \texttt{integral error} \\
D(t) &= \tfrac{G(t)-G(t-5)}{5} \quad \leftarrow \texttt{derivative} \\
I_p(t) &= K_0 i_d(t-5) + K_1 I_p(t-5) + K_2 I_p(t-10) \\
&\qquad \leftarrow \texttt{insulin on board feedback} \\
r(t) &= \begin{pmatrix} K_p(G(t) - G_0) + K_i I_e(t) + \\ K_d D(t) - \gamma I_p(t) \end{pmatrix} \\
&\qquad \leftarrow \texttt{raw control output} \\
u_c(t) &= \begin{cases} 0 & r(t) \le 0 \\ r(t) & 0 \le r(t) \le i_{max} \\ i_{max} & r(t) \ge i_{max} \end{cases} \\
&\qquad \leftarrow \texttt{saturated control output}
\end{aligned}
$$

Fig. 5: PID-based control with insulin feedback equations that govern the insulin delivered to the patient $u_c(t)$ based on the glucose input $G(t)$. The control law is based on parameters highlighted in blue. Brief explanations for each equation is also shown.

Each model provides a constraint that predicts a glucose range at a future time based on different parts of the past history. The models can be used to provide a predicted range over a time horizon. Figure 7 demonstrates the predicted ranges over time against the observed value over a test data set for patient ID 1 which was not used to fit the models used.

IV. Reachability Analysis

In this section, we discuss the use of the composite data-driven models inferred in the previous section to establish worst-case bounds over the range of BG values achieved by a given closed loop controller.

A. PID-Based Control Law

We will first briefly describe the PID-based control algorithm originally proposed by Steil et al [45], [48], [50]. This control algorithm has been extensively validated by clinical trials and is the basis of a commercially available closed-loop system [23].

Figure 5 shows the equations that govern the calculation of the current insulin input, $u_c(t)$, from the input glucose signal, $G(t)$. The controller is governed by parameters that include PID gains K_p: the proportional gain, K_i: the integral gain and K_d: the derivative gain. Other gains include the insulin feedback term gain γ. The controller also uses a maximum insulin delivery rate i_{max}. Weinzimer et al propose a basic rule of thumb for setting the gains using the daily insulin requirement of the patient [50]. We will describe these rules further in Section [V].

B. Reachability Analysis

Given a control law and the parameter values, we wish to compute the maximum/minimum possible values of glucose achieved by the data driven model under the action of the closed loop controller over a time horizon $t \in [0, T]$. Since the each data-driven model looks back over the historical glucose data for time Δ_G and insulin-on-board data for time Δ_I, we

need to define this history for the past time $[-\Delta, 0)$ before our analysis starts.

History Assumptions: We will make the assumption that the historical values belong to some set "reasonable" range for the glucose and insulin on board.

1) For all $t < 0$, $G(t) \in [G_{min}, G_{max}]$ wherein $G_{min} = 70$ mg/dL and $G_{max} = 180$ mg/dL
2) For all $t < 0$, $\mathrm{I}(t) \in [\mathrm{I}_{min}, \mathrm{I}_{max}]$ wherein $\mathrm{I}_{min} = 0.5$ U and $\mathrm{I}_{max} = 4.0$ U

As such, these assumptions capture an infinite set of possible histories before $t = 0$, when the controller is turned on. The reader may notice that we assume no violations are possible in the "near past" before the controller starts. This assumption allows us to ascribe any violations observed at times $t \gg 0$ as properties of the controller rather than (say) large insulin overdoses delivered before the controller was switched on.

Reachability Analysis Encoding: We will now discuss how to encode the reachability analysis. Let us assume that we have k models $M_1, \ldots, M_k$ with M_i described by the ARMAX law with delays $(\Delta_{G,i}, \Delta_{I,i})$ and confidence interval $[\ell_i, u_i]$.

$$G(t+\Delta_{G,i}) = a_{0,i}G(t)+a_{1,i}G(t-\Delta_{G,i})+b_i\mathrm{I}(t-\Delta_{I,i})+[\ell_i, u_i]\,.$$

The verification is run over a time horizon T with the control law run every $\Delta = 5$ minutes. We will assume that Δ divides $\Delta_{G,i}, \Delta_{I,i}$ for $i \in \{1, \ldots, k\}$ and also Δ divides T. Let $\Delta_{G,max} : \max(\Delta_{G,i})_{i=1}^{k}$ and $\Delta_{I,max} = \max(\Delta_{I,j})_{j=1}^{k}$.

Figure 6 outlines the overall optimization setup by first introducing the unknown variables and constraints that describe a valid execution of the overall closed loop over the time horizon T.

The goal of this optimization problem is to find the largest possible value of BG at time T provided by any execution that conforms to each of the models $M_1, \ldots, M_k$, and wherein the insulin inputs are generated according to the control law shown in Figure 5. Additionally, we provide constraints that link the IOB at time t with the past insulin infusion history, and provide a means to encode the saturation of the raw insulin term by $i_{\max}$ and 0 in the PID law (Fig. 5 last equation).

Recursive IOB: The link between IOB and insulin inputs is provided by (1). However, this requires a long history of past insulin values. We replace this by an "infinite impulse response" approximation provided by the equation

$$\mathrm{I}(t) = \begin{array}{c} 1.89\mathrm{I}(t-5) - 0.9\mathrm{I}(t-10)+ \\ \frac{1}{12}(u_c(t) - 0.9u_c(t-5) + 0.002u_c(t-10)) \end{array} . \quad (2)$$

Note that the recursive version assumes that the value of u_c is changed at 5-minute intervals.

Encoding Saturation: Another important aspect is the saturation of the raw feedback term $r(t)$ in Fig 5, such that $u_c(t)$ is clamped at 0 whenever $r(t) \leq 0$ and $u_c(t) = i_{max}$ whenever $r(t) \geq i_{max}$. This is a piecewise linear function which can be encoded by the addition of binary indicator variables, $w(t) \in \{0, 1\}$. Specifically, we use the constraints

$$C_1 : \; u_c(t) \geq r(t) \wedge \; C_2 : \; u_c(t) \geq 0 \wedge$$
$$C_3 : \; u_c(t) \leq r(t) + i_{max}w(t) \wedge$$
$$C_4 : \; u_c(t) \leq i_{max}(1 - w(t))$$

Real	$G(-\Delta_{G,max}), \ldots, G(-5)$	History Gluc.
	$\mathrm{I}(-\Delta_{I,max}), \ldots, \mathrm{I}(-5)$	History IOB.
	$G(0), G(5), \ldots, G(T)$	Glucose
	$\mathrm{I}(0), \mathrm{I}(5), \ldots, \mathrm{I}(T)$	IOB
	$u_c(0), u_c(5), \ldots, u_c(T)$	Insulin
	$I_e(0), I_e(5), \ldots, I_e(T)$	Integral Err.
	$I_p(0), I_p(5), \ldots, I_p(T)$	Ins. feedback
	$r(0), r(5), \ldots, r(T)$	Raw ins.
Binary	$w(0), w(5), \ldots, w(T)$	0-1 variables
maximize $G(T)$ minimize for lower bnd		
$G_{min} \leq G(t) \leq G_{max}$		$t < 0$
$\mathrm{I}_{min} \leq \mathrm{I}(t) \leq \mathrm{I}_{\max}$		Historical range
$G(t+\Delta_{G,i}) \leq a_{0,i}G(t) + a_{1,i}G(t-\Delta_{G,i} + b_i\mathrm{I}(t-\Delta_{I,i}) + u_i$		
$G(t+\Delta_{G,i}) \geq a_{0,i}G(t) + a_{1,i}G(t-\Delta_{G,i} + b_i\mathrm{I}(t-\Delta_{I,i}) + l_i$		
for all $t = 0, 5, \ldots, T, i = 1, \ldots, k$		Model M_i constr.
$\mathrm{I}(t) = F(u_d(t), u_d(t-5), \mathrm{I}(t-5), \mathrm{I}(t-10))$		IOB see (2)
$I_e(t) = I_e(t-5) + (G(t) - G_0)$		Integral error
$I_p(t) = K_0 i_d(t-5) + K_1 I_p(t-5) + K_2 I_p(t-10)$		IOB feedback
$r(t) = \left(\begin{array}{c} K_p(G(t) - G_0) + K_i I_e(t) + \\ K_d \frac{(G(t)-G(t-5))}{5} - \gamma I_p(t) \end{array} \right)$		Raw ctrl. output
$u_c(t) \geq r(t)$		
$u_c(t) \leq r(t) + i_{max}w(t)$		
$u_c(t) \leq i_{max}(1 - w(t))$		
$u_c(t) \geq 0$		Saturation

Fig. 6: Optimization problem for finding the maximum possible $G(T)$, wherein the constraints describe an execution of the closed loop according to the data-driven models $M_1, \ldots, M_k$ and PID control equations in Fig. 5 modified by encoding the saturation term using 0-1 variables.

Lemma 1. *The constraints $C_1, \ldots, C_4$ ensure that*

$$u_c(t) = \begin{cases} 0 & r(t) < 0 \\ r(t) & 0 \leq r(t) \leq i_{max} \\ i_{max} & o.w. \end{cases} .$$

Proof. Suppose $r(t) < 0$, we note that $w(t)$ must be 1. If $w(t) = 0$ for the sake of contradiction, then $C_2 : u_c(t) \geq 0$ conflicts with $C_3 : \; u_c(t) \leq r(t) + i_{max}0$. Therefore, if $r(t) < 0$, we may substitute 1 for $w(t)$. The constraints simplify to

$$C_2 : \; u_c(t) \geq 0 \; \wedge \; C_4 : \; u_c(t) \leq 0$$

In other words, $u_c(t)$ must be 0.

Suppose $r(t) > 0$, then we note that $w(t)$ must be 0. Otherwise, if $w(t)$ were 1, then $C_4 : u_c(t) \leq 0$ contradicts with $C_1 : u_c(t) \geq r(t)$. Substituting 0 for $w_c(t)$, we obtain

$$C_1 : u_c(t) \geq r(t) \; \wedge \; C_3 : \; u_c(t) \leq r(t) \; \wedge \; C_4 : \; u_c(t) \leq i_{max}$$

Now, we can also see that if $0 < r(t) < i_{max}$ then $u_c(t) = r(t)$. Else, if $r(t) \geq i_{max}$ then $u_c(t) = i_{max}$. □

Theorem 2. *The maximum (minimum) value of $G(T)$ obtained by solving the optimization problem in Figure 6 yields the largest (smallest) value of blood glucose at time T obtained by any closed loop execution compatible with the given models and control law.*

TABLE II: Table showing percent time in range actual patient data fits into our model estimated range for a sampling of patients along with the standard deviation measured across various bins.

Patient ID	Mean time in Range	std
001-0001	95.05%	±5.8%
001-0002	96.22%	±3.66%
002-0004	94.08%	±6.13%
001-0011	95.32%	±6.47%
002-0002	88.75%	±8.55%
001-0013	96.77%	±5.14%
002-0011	93.84%	±6.39%
004-0004	96.17%	±4.59%
002-0015	98.16%	±2.14%
001-0018	96.80%	±3.60%
002-0016	98.79%	±0.80%
002-0001	96.26%	±3.29%
001-0012	91.36%	±8.20%
001-0006	94.41%	±6.11%
001-0003	91.57%	±6.73%
002-0013	96.77%	±5.14%

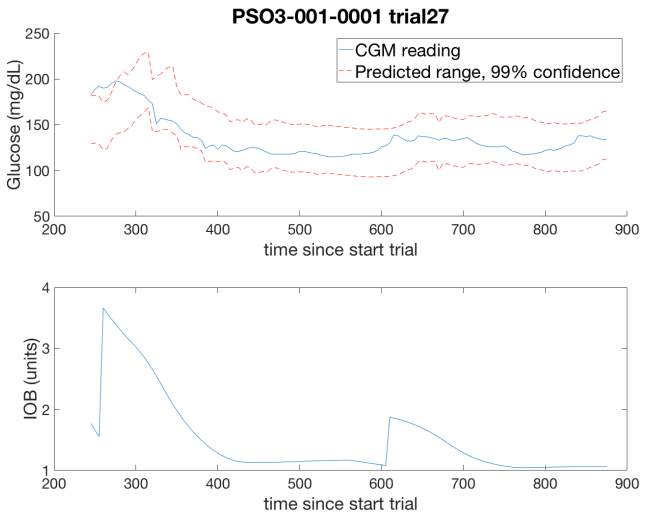

Fig. 7: Example of model predictions using our non-deterministic approach (dashed red) and actual patient blood glucose (solid blue) for patient ID 1.

V. Results and Discussion

In this section, we describe the overall results of our model fitting, reachability analysis, and the parameter tuning. The approach described thus far has been implemented using a combination of tools: (a) standard regression procedures available in Matlab(tm); (b) the integer linear programming tool Gurobi was used to perform reachability analysis and (c) the post processing was carried out using a combination of Python and R.

Model Fitting: The process of model fitting required us to run a single regression problems for time windows of $120, 180$ and 300 minutes. In order to section training and test data, we use k-fold cross-validation with $k = 8$, leading to 8 regression problems for each window. The overall model fitting took an average of 2 minutes/patient on a Macbook pro laptop. Once the models were obtained, we tested the goodness of fit to verify that the actual data point was inside the predicted range 95% of the time, in the manner of $k-$fold cross-validation. Fig. 7 presents an example bin with the predicted ranges juxtaposed over the actual values. Table II reports the fraction of data points that were inside the predicted range, averaged for each patient across all the bins considered. As expected, we observe that our model captures $95 \pm 2.72\%$ of the data points. However, we note that variations exist across patients and bins.

Reachability Analysis: As mentioned earlier, the reachability analysis was carried out using the state-of-the-art Gurobi ILP solver [21]. On average, each reachability analysis run for a single patient and bin required 0.6 minutes of running time. Full reachability analysis over all bins and all patients was performed for both the "out of the box" and our improved tuning rule settings. We observed that most of the parameters across bins were very close to each other. Thus, to reduce analysis burden when searching the space for "best" control parameter, we averaged the model coefficients to produce three representative sets of models or each patient and performed reachability analysis on these averaged models. Our identified tuning law is based on these averaged results, however it was tested on all bins and all patients. This significantly reduced computational time as running the parameter search step across all bins for each patient would have required nearly $30days$ of CPU time on a single core.

Figure 8 depicts the results of the reachability analysis for representative patients/bins.

A. Tuning Control Parameters

We will now investigate the use of the overall framework for examining how patients perform under different values of the parameters. Following the tuning rule proposed in the original PID controller, we focus on tuning the proportional gain K_p. Once K_p is set, the value of integral gain is set to $K_i = K_p T_i$ and derivative gain $K_d = K_p/T_d$, following Steil et al [45], [48], [50]. Furthermore, the original rule for K_p [50] is

$$K_p : \frac{\text{Daily Insulin}}{135}.$$

Using this tuning rule, our analysis predicts that 38 out of 44 patients analyzed are free of hyper-glycemia. However, only 2 out of 44 patients are free of the possibility of hypo-glycemia. Figure 8(a) shows an example of a patient/bin wherein we observe convergence of the range of possible glucose values into the euglycemic range, whereas Figure 8(b) depicts a patient whose blood glucose values fail to settle.

Fig. 9 plots the lower and upper bounds for patients sorted by their K_p values (and thus the daily insulin requirement).

Improving the Controller Tuning. To improve the controller tuning, we explore for different values of K_p for each patient (keeping the relation between K_p, K_i and K_d as originally specified by Weinzimer et al [50]). Therefore,

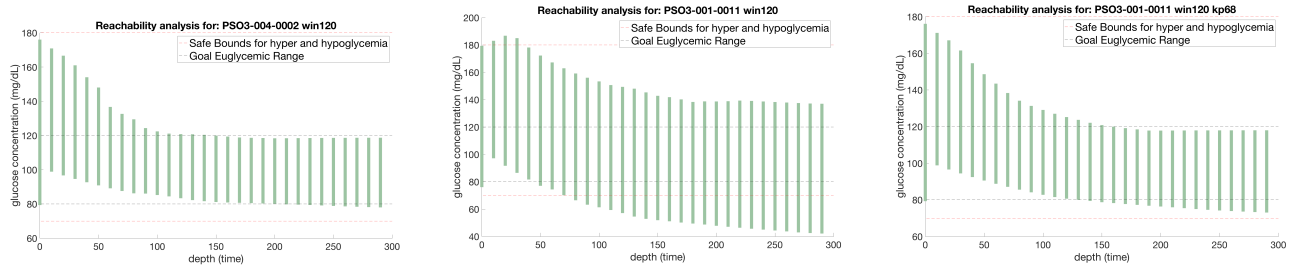

(a) **(b)** **(c)**

Fig. 8: Reachability analysis plots showing ranges of glucose values across time for chosen patients and bins. (a) Original tuning that works well; (b) Original tuning that works poorly; and (c) results of improved tuning for the patient and bin in (b).

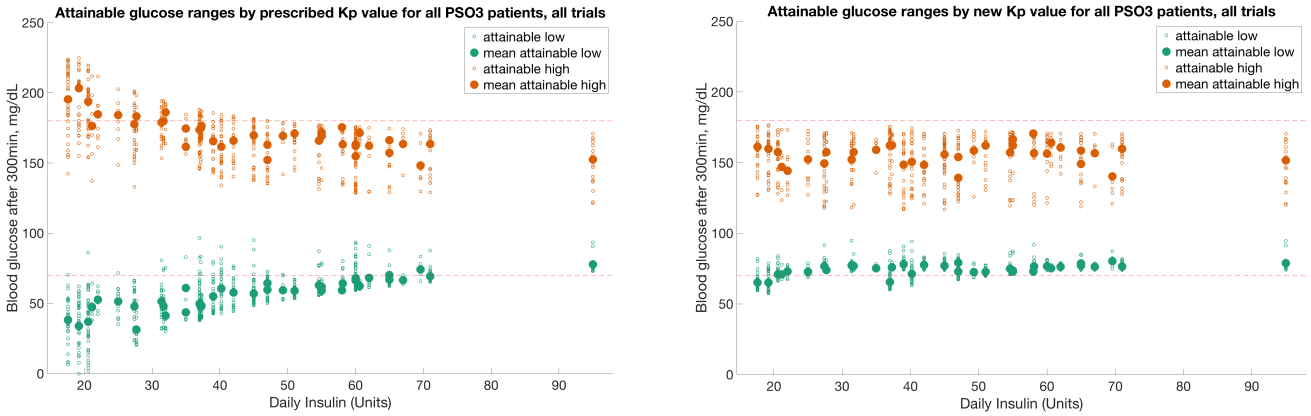

(a) **(b)**

Fig. 9: Bounds on reachable BG levels for patients sorted by their daily insulin requirements: **(a)** original tuning rule and **(b)** improved tuning rule suggested by reachability analysis and regression. Open circles denote each bin for each patient, filled circles denote mean values across all bins for each patient.

for each patient, we explore seven evenly distributed values in the range $[K_0, 0.8]$, where $K_0 = K_{p0}$ (same as the original tuning) if this original tuning was unsafe, and otherwise, $K_0 = K_{p0} - 0.1$. We select the value of K_p that provides the optimal performance in terms of (a) choose all parameter values that avoid hyperglycemia; (b) from this set, we choose all parameter sets that avoid hypoglycemia; and (c) choose the smallest K_p as the final result. The value of K_p discovered for each patient is provided in the appendix (Table IV).

Next we search for a tuning rule using the optimal values returned by the search procedure. To do this, we set aside a test group consisting of 5 patients and on the remaining patients, we perform linear regression to estimate the optimal K_p value as a function of the daily insulin requirement and HbA1C values of the patient. Doing so suggests the following tuning rule:

$$K_p^r = \begin{cases} (0.52\text{HbA1c} + 0.036)\frac{\text{DailyInsulin}}{135} & \text{if HbA1c} \leq 7 \\ (-0.08\text{HbA1c} + 2.24)\frac{\text{DailyInsulin}}{135} & \text{otherwise} \end{cases}.$$

However, the formula estimates a larger K_p value than the results of our search procedure for 4 out of 44 patients.

Time Spent in Category	**Original Tuning Rule** mean (std)	**New Tuning Rule** mean (std)
Safe Range 70 − 180mg/dL	14.80% (21.60%)	84.77% (26.54%)
Severe Hypoglycemia BG< 50mg/dL	29.14% (33.36%)	0% (0%)
Hypoglycemia BG< 70mg/dL	85.12% (21.56%)	15.23% (26.54%)
Hyperglycemia BG> 250mg/dL	0% (0%)	0% (0%)

TABLE III: Changes in time-in-range percentages between out-of-the-box tuning rule and our new tuning rule.

Therefore, we set $K_p^{\max} = 0.74$ as a higher limit for K_p, I.e., $K_p : \max(K_p^{\max}, K_p^r)$. Figure 9 show the improved bounds wherein 82% of the patients (as opposed to 5% of the patients) are now within bounds. Bounds are improved for each bin and each patient, as seen in the open dots, as well as for the means (closed dots). Also, Figure 8(c) shows the improvement to a specific patient/bin under the new tuning rules, wherein Figure 8(b) shows the reachability results under the older rule.

Full statistics on improved time-in-range between tuning

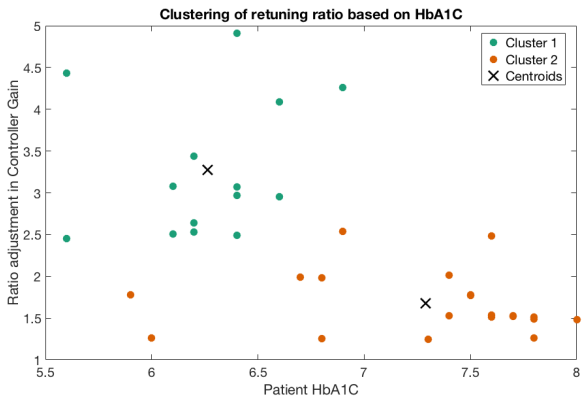

Fig. 10: Ratio of K_p from suggested tuning rule versus original rule clustered by patient HbA1C.

rules given in Table III.

Figure 10 plots the ratio of the K_p values under the new tuning rule versus the original K_p value against the patient's HbA1C. We find that for individuals with HbA1C$>$ 7, the original approach requires much less of a change than for individuals with HbA1C ≤ 7. These results are confirmed from a 2-means clustering. A Kolmogorov-Smirnof test confirms that the two groups are "significantly" different ($p = 0.0015$).

In other words, HbA1C is a strong predictor of performance under the original tuning rule. This pattern conforms to clinical experience: patient trials for the AP have used individuals with high HbA1C (HbA1C $= 7.7 \pm 0.84$) due to significantly worse control performance being observed for those with HbA1C near 6 [19].

B. Limitations and Threats to Validity

We will briefly describe the threats to validity of our approach and steps taken to mitigate against these threats. Broadly, the threats can be partitioned into three categories: (a) threats to the assumptions made in our modeling approach; (b) threats arising from the nature of the dataset used; and (c) threats due to limited information available about the implementation of the PID control law.

Section III carefully outlines many of the assumptions made, providing a measure of justification. The assumption of linearity is fundamental to our modeling approach. However, it cannot be justified unless we carefully compare our approach with other models for the same problem. This will form part of our future work. The use of insulin-on-board is quite common in many artificial pancreas systems. However, this calculation is made using a single formula for all patients, rather than using a patient specific approach. Next, the choice of $p = 2, q = 1$ for the glucose history is justified by studying the autocorrelations. However, the choices for the various timing delays and number of such delays are made using population level knowledge about insulin action rather than any insights drawn from the data.

The nature of the dataset imposes limitations and therefore, threats to validity. First of all, our approach is limited to nighttime data: we do not have information on meals or exercise, which are typically daytime activities. Also, we drop bins that involve rescue carbohydrates. This biases our models in terms of the range of BG values used to train our models. This bias is hard to overcome since hypoglycemia is a serious clinical emergency and as such, requires immediate intervention. Clinical studies of patient behavior under hypoglycemia run the risk of serious harm to the patient.

A final threat lies in our modeling of the control law. Currently, our models are reconstructed from equations provided in the relevant papers [45], [48], [50]. However, it is a well known fact that controller implementations incorporate safety features around the core control law: one such feature could be a mechanism to shut off the controller if hypoglycemia is predicted. Such mechanisms could in fact make our reachability analysis more pessimistic than what will be seen in practice. Indeed, clinical evidence on the performance of PID-based systems strongly indicates this possibility [19].

VI. Related Work

We have already discussed the background related to AP controllers and modeling of insulin-glucose regulation. We restrict the discussion to closely related data driven approaches.

Personalized control has been recognized as an important area for the artificial pancreas. Model Predictive Control (MPC) algorithms provide for personalization by learning model parameters from patient data. Hovorka et al propose a nonlinear MPC scheme that updates the parameters of the model periodically using the patient data [24], [25]. Dassau et al use a data driven approach to derive plant models that are used to construct an explicit MPC system [15]. Ghorbani et al present a data-driven modeling approach using fractional calculus and use their models to derive control strategies for mitigating hypoglycemia [20]. Capel et al. evaluate a rule-based approach that is based on training a neural network model that predicts the future course of the patient glucose values. This network is trained from historical data collected from the patient [29]. To address patient safety concerns, these approaches place limits on the insulin-on-board for the patient. However, all of these approaches fail to account for the uncertainty in the system identification process. The recent work of Paoletti et al uses a robust MPC scheme that accounts for meal uncertainties but uses a deterministic patient model with numerous parameters that are hard to estimate without highly intrusive lab measurements on the patient [42].

Abbas et al present a data-driven approach for testing and comparing the performance of algorithms for arrythmia detection and discrimination algorithms for implantable cardioverted defibrillators [1]. Their approach uses a probabilistic generative model for various types of arrythmias learned from patient data. As such, the goal of this paper is also similar: use data-driven models to analyze the performance of control algorithms in physiological closed loops. A key difference beyond the application domain is that our approach models a closed loop system wherein the data-driven model is in a closed loop with a controller. In contrast, the approach of

Abbas et al is open loop wherein the data driven model drives the control algorithms, but its decisions do not affect the inputs to the model.

Fan et al recently presented a data-driven verification approach that learns sensitivity information from simulation traces to drive time bounded verification of automotive models. Here we distinguish between a simulation-based black-box approach, wherein simulations can be run on chosen initial states and control inputs through an existing (black-box) model versus an approach such as ours that learns a model from available data [17]. Also, the available clinical data is often incomplete and noisy in contrast to simulations.

VII. Conclusion and Future Directions

Thus, we have presented a data-driven modeling approach along with reachability analysis of closed loop PID controller. We derive simple rule of thumb whose effectiveness can be evaluated clinically. As part of our future work, we plan to make our approach more robust by running on larger datasets that include daytime data as well. For this, we anticipate adjusting model parameters based on time-of-day, due to variability in hormones, food, etc. We also hope to work with clinicians to use the data driven approach to make clinical trials of future devices easier. Finally, the models derived by our approach can be used to design controllers that use data-driven models on the fly for predicting safe control inputs.

Acknowledgments: The authors thank Sydney L. Kennan for contributing to a preliminary version of this paper; Faye Cameron, and Greg Forlenza for helpful discussions. This research was funded by the NSF under award # 1446900. All opinions expressed are those of the authors and not necessarily of the NSF.

References

[1] H. Abbas, Z. Jiang, K. Jang, J. Liang, S. Dixit, and R. Mangharam. Computer aided clinical trials for implantable cardiac devices. *SES 2016: Symposium F-2*, 2016.

[2] H. Akaike. A new look at the statistical model identification. *IEEE Trans. on Automatic Control*, 19(6):716–723, 1974.

[3] E. Atlas, R. Nimri, S. Miller, E. A. Grunberg, and M. Phillip. MD-Logic artificial pancreas system: A pilot study in adults with type 1 diabetes. *Diabetes Care*, 33(5):1072–1076, May 2010.

[4] B. W. Bequette. Algorithms for a closed-loop artificial pancreas: The case for model predictive control. *J. Diabetes Science and Technology*, 7:1632–1643, November 2013.

[5] R. M. Bergenstal, S. Garg, and *others*. Safety of a hybrid closed-loop insulin delivery system in patients with type 1 diabetes. *JAMA Letters*, pages E1–E2, 2016.

[6] F. Cameron, G. Fainekos, D. M. Maahs, and S. Sankaranarayanan. Towards a verified artificial pancreas: challenges and solutions for runtime verification. *Lecture Notes in Computer Science*, 9333:2–17, 2015.

[7] F. Cameron, G. Niemeyer, and B. W. Bequette. Extended multiple model prediction with application to blood glucose regulation. *J. Process Control*, 22(8):1422–1432, Sep 2012.

[8] F. Cameron, D. M. Wilson, B. A. Buckingham, and *others*. Inpatient studies of a kalman-filter-based predictive pump shutoff algorithm. *J. Diabetes Science and Technology*, 6(5):1142–1147, 2012.

[9] A. Chakrabarty, S. Zavitsanou, F. J. D. III, and E. Dassau. Event-triggered model predictive control for embedded artificial pancreas systems. *IEEE Trans. on Biomedical Engg.*, 2017.

[10] H. P. Chase and D. Maahs. *Understanding Diabetes (Pink Panther Book)*. Children's Diabetes Foundation, 12 edition, 2011. Available online through CU Denver Barbara Davis Center for Diabetes.

[11] F. Chee and T. Fernando. *Closed-Loop Control of Blood Glucose*. Springer, 2007.

[12] C. Cobelli, D. Foster, and G. Toffolo. *Tracer Kinetics in Biomedical Research*. Springer Science & Business Media, 2000.

[13] C. Dalla Man, M. Camilleri, and C. Cobelli. A system model of oral glucose absorption: validation on gold standard data. *IEEE Trans. on Biomedical Engg.*, 53(12):2472–2478, 2006.

[14] C. Dalla Man, D. M. Raimondo, R. A. Rizza, and C. Cobelli. Gim, simulation software of meal glucoseinsulin model, 2007.

[15] E. Dassau, H. Zisser, H. R.A., and *others*. Clinical evaluation of a personalized artificial pancreas. *Diabetes Care*, 36(4):801–9, 2013.

[16] F. H. El-Khatib, S. J. Russell, D. M. Nathan, R. G. Sutherlin, and E. R. Damiano. A bihormonal closed-loop artificial panceras for type 1 diabetes. *Sci. Transl. Med.*, 2, April 2010.

[17] C. Fan, B. Qi, S. Mitra, and M. Viswanathan. *DryVR: Data-Driven Verification and Compositional Reasoning for Automotive Systems*, pages 441–461. Springer, 2017.

[18] G. P. Forlenza, S. Deshpande, T. T. Ly, and *others*. Application of zone model predictive control artificial pancreas during extended use of infusion set and sensor: A randomized crossover-controlled home-use trial. *Diabetes Care*, 2017.

[19] S. K. Garg, S. A. Weinzimer, W. V. Tamborlane, B. A. Buckingham, and *others*. Glucose outcomes with the in-home use of a hybrid closed-loop insulin delivery system in adolescents and adults with type 1 diabetes. *Diabetes Technology and Therapeutics*, 19(3):1–9, 2017.

[20] M. Ghorbani and P. Bogdan. Reducing risk of closed loop control of blood glucose in artificial pancreas using fractional calculus. In *36th Annual International Conference of the IEEE Engineering in Medicine and Biology Society (EMBS)*, pages 4839–4842, Aug 2014.

[21] Gurobi Optimization, Inc. Gurobi optimizer reference manual, 2016.

[22] D. M. Hamby. A review of techniques for parameter sensitivity analysis of environmental models. *Environmental Monitoring Assessment*, 32(2):135–154, September 1994.

[23] Hooman Hakami (Medtronic Inc.). FDA approves MINIMED 670G system - world's first hybrid closed loop system.

[24] R. Hovorka, J. M. Allen, D. Elleri, and *others*. Manual closed-loop delivery in children and adoloscents with type 1 diabetes: a phase 2 randomised crossover trial. *Lancet*, 375:743–751, February 2010.

[25] R. Hovorka, V. Canonico, L. Chassin, and *others*. Nonlinear model predictive control of glucose concentration in subjects with type 1 diabetes. *Physiological Measurement*, 25:905–920, 2004.

[26] R. Hovorka, F. Shojaee-Moradie, and *others*. Partitioning glucose distribution/transport, disposal and endogenous production during IVGTT. *Am. J. Physiol. Endocrinol. Metab.*, 282:992–1007, 2002.

[27] C.-M. Huang, C.-J. Huang, and M.-L. Wang. A particle swarm optimization to identifying the armax model for short-term load forecasting. *IEEE Trans. on Power Systems*, 20(2):1126–1133, May 2005.

[28] F. J. D. III, L. M. Huyett, J. B. Lee, H. C. Zisser, and E. Dassau. Closed-loop artificial pancreas systems: Engineering the algorithms. *Diabetes Care*, 37(5):1191–1197, May 2014.

[29] Ismael Capel et al. Artificial pancreas using a personalized rule-based controller achieves overnight normoglycemia in patients with type 1 diabetes. *Diabetes Technology Therapeutics*, 16(3):172–9, March 2014.

[30] L. Kovacs, P. Szalay, T. Ferenci, J. Sapi, P. Sas, D. A. Drexler, I. Harmati, B. Benyo, and A. Kovacs. Model-based control algorithms for optimal therapy of high-impact public health diseases. *Intelligent Engineering Systems (INES)*, pages 531–536, 2012.

[31] J. N. Kutz, S. L. Brunton, B. W. Brunton, and J. L. Proctor. *Dynamic Mode Decomposition: Data-Driven Modeling of Complex Systems*. Society for Industrial and Applied Mathematics, 2016.

[32] E. Lehmann and T. Deutsch. A physiological model of glucose-insulin interaction in type 1 diabetes mellitus. *J. biomedical engineering*, 14(3):235–242, 1992.

[33] J. Liepe, P. Kirk, S. Filippi, T. Toni, C. P. Barnes, and M. P. H. Stumpf. A framework for parameter estimation and model selection from experimental data in systems biology using approximate bayesian computation. *Nature Protocols*, 9(2):439–456, January 2014.

[34] D. M. Maahs, P. Calhoun, B. A. Buckingham, and Others. A randomized trial of a home system to reduce nocturnal hypoglycemia in type 1 diabetes. *Diabetes Care*, 37(7):1885–1891, July 2014.

[35] C. D. Man, F. Micheletto, D. Lv, M. Breton, B. Kovatchev, and C. Cobelli. The uva/padova type i diabetes simulator: New features. *J. Diabetes Science and Technology*, 8(1):26–34, 2014.

[36] C. D. Man, R. A. Rizza, and C. Cobelli. Meal simulation model of the glucose-insulin system. *IEEE Trans. on Biomedical Engg.*, 1(10):1740–1749, 2006.

[37] N. M. Mangan, S. L. Grunton, J. L. Proctor, J. N. Kutz, and S. L. Brunton. Inferring biological networks by sparse identification of nonlinear dynamics. *IEEE Trans. on Molecular, Biological and Multi-Scale Communications*, 2(1):52–63, 2016.

[38] N. M. Mangan, J. N. Kutz, S. L. Brunton, and J. L. Proctor. Model selection for dynamical systems via sparse regression and information criteria. *preprint*, 2017.

[39] D. Matthews, J. Hosker, A. Rudenski, B. Naylor, D. Treacher, and R. Turner. Homeostasis model assessment: insulin resistance and β-cell function from fasting plasma glucose and insulin concentrations in man. *Diabetologia*, 28(7):412–419, 1985.

[40] A. I. McLeod and W. K. Li. Diagnostic checking arma time series models using squared-residual autocorrelations. *J. Time Series Analysis*, 4(4):1467–9892, 1983.

[41] OpenAPS.org. Openaps project reference implementation. Cf. openaps. org, last accessed August 2017.

[42] N. Paoletti, K. Sum Liu, S. Smolka, and S. Lin. Data-driven robust control for type 1 diabetes under meal and exercise uncertainties. To Appear, CMSB 2017.

[43] S. Patek, B. Bequette, M. Breton, B. Buckingham, E. Dassau, F. Doyle III, J. Lum, L. Magni, and H. Zisser. In silico preclinical trials: methodology and engineering guide to closed-loop control in type 1 diabetes mellitus. *J Diabetes Sci Technol.*, 3(2):269–82, 2009.

[44] S. H. Rudy, S. L. Brunton, J. L. Proctor, and J. N. Kutz. Data-driven discovery of partial differential equations. *Science Advances*, 3(4):e1602614, 2017.

[45] J. L. Ruiz, J. L. Sherr, and *others*. Effect of insulin feedback on closed-loop glucose control: a crossover study. *J. Diabetes Science and Technology*, 6(5):1123–1130, 2012.

[46] S. Sankaranarayanan, C. Miller, R. Raghunathan, H. Ravanbakhsh, and G. Fainekos. A model-based approach to synthesizing insulin infusion pump usage parameters for diabetic patients. *Proc of 50th annual allerton conference on communication, control, and computing*, 2012.

[47] J. S. Skyler (editor). *Atlas of Diabetes: Fourth Edition*. Springer Science+Business Media, 2012.

[48] G. Steil, A. Panteleon, and K. Rebrin. Closed-sloop insulin delivery - the path to physiological glucose control. *Advanced Drug Delivery Reviews*, 56(2):125–144, 2004.

[49] G. M. Steil. Algorithms for a closed-loop artificial pancreas: The case for proportional-integral-derivative control. *J. Diabetes Sci. Technol.*, 7:1621–1631, November 2013.

[50] S. Weinzimer, G. Steil, K. Swan, J. Dziura, N. Kurtz, and W. Tamborlane. Fully automated closed-loop insulin delivery versus semiautomated hybrid control in pediatric patients with type 1 diabetes using an artificial pancreas. *Diabetes Care*, 31:934–939, 2008.

[51] M. Wilinska, L. Chassin, C. L. Acerini, J. M. Allen, D. Dunber, and R. Hovorka. Simulation environment to evaluate closed-loop insulin delivery systems in type 1 diabetes. *J. Diabetes Science and Technology*, 4, January 2010.

APPENDIX

A. Additional Tables

TABLE IV: The value of gain K_p original setting (old), value required to avoid hyper and/or hypo glycemia, ordered by increasing HbA1C. We observe that retuning ratio ($R = \frac{newGain}{oldGain}$) increases with lower HbA1C, indicating original tuning rule will poorly control patients with low HbA1C levels.

PtID	K_p **(old)**	K_p**(hyper)**	K_p**(hypo)**	**R**	**HbA1C**
002-0001	0.23	0.35	0.57	2.45	5.6
002-0011	0.14	0.21	0.63	4.43	5.6
004-0004	0.35	0.44	0.62	1.78	5.9
001-0012	0.45	0.58	0.58	1.26	6.0
001-0006	0.25	0.39	0.65	2.51	6.1
002-0002	0.19	0.28	0.57	3.07	6.1
001-0003	0.16	0.24	0.56	3.43	6.2
001-0005	0.24	0.36	0.60	2.53	6.2
004-0007	0.23	0.34	0.62	2.64	6.2
004-0006	0.13	0.20	0.64	4.90	6.4
002-0003	0.21	0.31	0.63	3.07	6.4
001-0004	0.22	0.33	0.66	2.97	6.4
001-0001	0.29	0.44	0.72	2.49	6.4
001-0016	0.16	0.24	0.64	4.08	6.6
002-0006	0.20	0.30	0.60	2.95	6.6
004-0003	0.31	0.46	0.62	1.99	6.7
001-0002	0.33	0.49	0.66	1.98	6.8
002-0012	0.53	0.66	0.66	1.25	6.8
001-0011	0.27	0.42	0.70	2.54	6.9
002-0004	0.15	0.22	0.65	4.23	6.9
002-0008	0.48	0.60	0.60	1.24	7.3
002-0014	0.29	0.45	0.60	2.01	7.4
001-0008	0.44	0.68	0.68	1.53	7.4
001-0017	0.35	0.44	0.62	1.78	7.5
004-0001	0.37	0.47	0.67	1.77	7.5
002-0005	0.27	0.34	0.68	2.48	7.6
002-0010	0.43	0.54	0.65	1.51	7.6
004-0005	0.36	0.46	0.56	1.53	7.6
001-0010	0.44	0.68	0.68	1.53	7.7
001-0018	0.41	0.51	0.62	1.52	7.7
001-0013	0.44	0.56	0.56	1.26	7.8
002-0015	0.43	0.54	0.65	1.51	7.8
002-0016	0.45	0.56	0.67	1.49	7.8
001-0013	0.44	0.56	0.56	1.26	7.8
002-0013	0.40	0.50	0.60	1.48	8